Adenosine Diphosphate (ADP)-Ribosylation of the Guanosine Triphosphatase (GTPase) Rho in Resting Peripheral Blood Human T Lymphocytes Results in Pseudopodial Extension and the Inhibition of T Cell Activation

By Darren G. Woodside, David K. Wooten, and Bradley W. McIntyre

From the Department of Immunology, University of Texas M.D. Anderson Cancer Center, Houston, Texas 77030

Summary

Scrape loading *Clostridium botulinum* C3 exoenzyme into primary peripheral blood human T lymphocytes (PB T cells) efficiently adenosine diphosphate (ADP)-ribosylates and thus inactivates the guanosine triphosphatase (GTPase) Rho. Basal adhesion of PB T cells to the β1 integrin substrate fibronectin (Fn) was not inhibited by inactivation of Rho, nor was upregulation of adhesion using phorbol myristate acetate (PMA; 10 ng/ml) or Mn^{++} (1 mM) affected. Whereas untreated PB T cells adherent to Fn remain spherical, C3-treated PB T cells extend F-actin–containing pseudopodia. Inactivation of Rho delayed the kinetics of PMA-dependent PB T cell homotypic aggregation, a process involving integrin αLβ2. Although C3 treatment of PB T cells did not prevent adhesion to the β1 integrin substrate Fn, it did inhibit β1 integrin/CD3-mediated costimulation of proliferation. Analysis of intracellular cytokine production at the single cell level demonstrated that ADP-ribosylation of Rho inhibited β1 integrin/CD3 and CD28/CD3 costimulation of IL-2 production within 6 h of activation. Strikingly, IL-2 production induced by PMA and ionomycin was unaffected by C3 treatment. Thus, the GTPase Rho is a novel regulator of T lymphocyte cytoarchitecture, and functional Rho is required for very early events regulating costimulation of IL-2 production in PB T cells.

Key words: integrins • cytoskeleton • interleukin 2 • cell adhesion • extracellular matrix

The actin cytoskeleton is clearly important in the regulation of T lymphocyte activity at a variety of different levels. A number of cell surface proteins involved in T cell function are associated with cytoskeletal complexes, including integrin receptors of the β1 and β2 subfamilies (1), CD45 (2, 3), CD2, CD4, CD8, CD44, class I MHC (4), and the ζ chain of the TCR–CD3 complex (5–7). As such, an intact cytoskeleton is essential for sustained signals required for T cell activation and may be necessary for TCR aggregation (8), as well as the spatial redistribution of cell surface molecules at the contact site between antigen-presenting cells and T cells (9). The role of the actin cytoskeleton is emerging as not just a conglomeration of protein subunits maintaining cell shape, but rather, as a highly coordinated molecular array providing a scaffold for the spatial distribution of mechanistic and signaling components requisite for physiologic function of T lymphocytes.

Key regulators of the actin cytoskeleton involve small GTPases of the Rho family. These include RhoA, RhoB, RhoC, RhoD, RhoE, Cdc42, TC10, G25K, Rac1, and Rac2 (for review see references 10, 11). Rho proteins are biochemical switches that when in the GTP-bound state regulate diverse biological phenomenon ranging from morphological changes to cytokinesis and gene induction. C3 exoenzyme from *Clostridium botulinum* specifically inhibits Rho activity, and not that of Rac or Cdc42 proteins, by adenosine diphosphate (ADP)[1]-ribosylating Rho on Asn^{41} (12) of the Rho effector domain. By using this Rho-specific inactivator, it has been demonstrated in leukocytes that Rho activity is required for B cell homotypic aggregation (13) and chemokine-induced adhesion (14), neutrophil migration and upregulated adhesion (14–16), NK cell mobility and cytolytic activity (17, 18), and the maintenance of monocyte morphology (19, 20). Recently, thymus-targeted C3 transgenic mice have been developed that demonstrate markedly decreased thymic mass and decreased numbers of mature T cells (21). In contrast, no studies to date have addressed the function of Rho in regulation of human peripheral blood T lymphocyte (PB T cell)

[1]*Abbreviations used in this paper:* 4,5-PIP_2, phosphatidylinositol 4,5-bisphosphate; ADP, adenosine diphosphate; Fn, fibronectin; GTP, guanosine triphosphatase; PB, peripheral blood; PIP 5-kinase, phosphatidylinositol 4-phosphate 5-kinase; PLC, phospholipase C.

 J. Exp. Med. © The Rockefeller University Press • 0022-1007/98/10/1211/11 $2.00
Volume 188, Number 7, October 5, 1998 1211–1221
http://www.jem.org

activation or in the regulation of the actin cytoskeleton. We have used the Rho-specific inactivator, C3 exoenzyme (12), to demonstrate the requirement of functional Rho in homotypic aggregation, maintenance of cell shape, and finally, in the costimulation of proliferation and IL-2 production in primary PB T cells.

Materials and Methods

Reagents. PMA, ionomycin, poly-L-lysine, and TRITC-phalloidin were purchased from Sigma Chemical Co. (St. Louis, MO). Fibronectin (Fn) was affinity purified from 200 ml of human plasma (Gulf Coast Regional Blood Center, Houston, TX) according to Hynes (22). Fn purity was determined by SDS-PAGE. Ig from the anti-CD3 mAb OKT3 hybridoma was purified from ascites. Anti-β1 integrin mAb 33B6 and anti-α4β1 integrin mAb 19H8 were generated in this laboratory and have been previously described (23, 24). The anti-αLβ2 mAb 85G1 was generated in this laboratory. mAbs rat anti–human IL-2–PE (IgG2a), anti–CD4-Cychrome (IgG1), control rat IgG2a-PE, and control IgG1-Cychrome were all purchased from PharMingen (San Diego, CA). Anti-CD28 mAb Leu28 and anti-αβ-TCR mAb were purchased from Becton Dickinson Immunocytometry Systems (San Jose, CA).

Cells. The T cell line J45.01 (American Type Culture Collection, Rockville, MD) was maintained in complete media (RPMI-1640 supplemented with 10% FBS, 10 U/ml of both penicillin and streptomycin; and 1 mM L-glutamine; all from GIBCO BRL, Gaithersburg, MD). Purified T cells were obtained by negative selection as previously described (25). In brief, mononuclear cells were isolated from the buffy coats (Gulf Coast Regional Blood Center) of healthy donors by density-dependent cell separation on Ficoll-Hypaque (1.077 g/ml; Amersham Pharmacia Biotechnology Inc., Piscataway, NJ). Monocytes were removed by several rounds of plastic adherence on tissue culture–treated petri dishes (Corning Glass Works, Corning, NY) for 45 min at 37°C and 5% CO_2. Further density dependent cell separation was performed on discontinuous percoll (295 mOsm; Sigma Chemical Co.) gradients (44, 48, and 60% vol/vol percoll in RPMI-1640; GIBCO BRL) to remove residual monocytes, PMNs, and red blood cells. The 48%/60% interface layer was carefully collected, washed in RPMI-1640, and then B lymphocytes were removed by adherence to nylon wool (Polysciences Inc., Warrington, PA) columns for 45 min at 37°C and 5% CO_2. The resultant lymphocyte population was routinely >95% $CD3^+$ as determined by flow cytometric analysis (Epics Profile; Coulter Immunology, Hialeah, FL). Purified T cells were maintained in complete media and used within 24 h of isolation.

Western Blotting. Cell lysates from $\sim 2 \times 10^6$ cell equivalents (J45.01) or 3×10^6 cell equivalents (PB T cells) were subjected to 12.5% SDS-PAGE and transferred to polyvinylidene difluoride (PVDF) membranes (Bio-Rad Laboratories, Hercules, CA). The following Western blotting steps were carried out at 4°C for at least 2 h. PVDF membranes were blocked with 5% BSA and 5% nonfat milk in TBS/Tween (10 mM Tris-HCl, pH 8.0, 150 mM NaCl, and 0.05% Tween-20) after transfer from gels. Membranes were extensively washed and then incubated with the primary (0.5 μg/ml) goat anti–RhoA polyclonal antibody (Santa Cruz Biotechnology, Santa Cruz, CA). After washing, membranes were incubated with goat anti–rabbit HRP (Cappel Laboratories, Malvern, PA). Chemiluminescence was performed as described by the manufacturer (Pierce Chemical Co., Rockford, IL).

Cell Adhesion Assays. Adhesion assays were performed in modified Tyrodes buffer (26) composed of 12 mM $NaHCO_3$, pH 7.4, 150 mM NaCl, 2.5 mM KCl, 2 mM $MgCl_2$, 1 mg/ml BSA, and 1 mg/ml glucose. Plates were precoated with Fn (10 μg/ml) for at least 2 h at room temperature in 0.1 M $NaHCO_3$. BSA (2% wt/vol) was then added to block unbound sites. Cells were resuspended in modified Tyrodes buffer alone or in modified Tyrodes buffer containing PMA (10 ng/ml) or Mn^{++} (1 mM). After 1×10^5 cells were added to the washed plates in 100 μl of modified Tyrodes, plates were spun at 300 rpm for 5 min and then incubated for 45 min at 37°C and 5% CO_2. Two digitized images captured as described in Szabo et al. (27) were analyzed using National Institutes of Health Image software (available from ftp://codon.nih.gov/pub/nih-image/nih-image161_fat.hqx) from each well before washing and then plates were carefully washed 4× with prewarmed (37°C) modified Tyrodes buffer. After washing, images from the prewash position were analyzed again. Cell numbers were quantitated using NIH Image software and adhesion assays are graphed as the percentage of input cells remaining after washing.

Quantitation of Cell Morphology. Quantitation of cell morphology by digital image analysis was performed as described previously (27). Images of Fn adherent cells (obtained from the same cells used in the adhesion assays described above) were digitized and analyzed with NIH Image software. Dividing the theoretical maximum area for a given perimeter ($perimeter^2/4\pi$) by the observed area provides a spreading index where absolute roundness is 1.0 (27). Any deviation from roundness gives a spreading index >1.0. Random fields of adherent cells were captured from various treatment groups and the spreading index quantitated. A percent change from roundness was calculated according to the following formula: % change = ([morphological index C3 treated − 1.0]/[morphological index C3 control − 1.0]) × 100.

Intracellular Incorporation of Macromolecules into Freshly Isolated PB T Lymphocytes. C3 was scrape loaded into freshly isolated PB T lymphocytes. Bacteriological petri dishes (35 mm; Becton Dickinson Labware (Lincoln Park, NJ) were coated with the nonspecific cell attachment factor poly-L-lysine (10 μg/ml) in PBS for at least 2 h at room temperature and then blocked with 1% (wt/vol) BSA for 30 min at room temperature. Cells were washed 4× in RPMI-1640 and resuspended at 10×10^6 cells/ml in RPMI-1640. These cells were plated ($<15 \times 10^6$ cells/dish) onto PBS washed poly-L-lysine dishes and incubated for 30 min at 37°C. After incubation, supernatants were removed and at least 200 μl of prewarmed (37°C) RPMI-1640 containing C3 (50 μg/ml) or appropriate controls were gently layered over the cells. After further incubation for 5 min at 37°C, cells were physically removed from the surface with a cell scraper (Costar, Cambridge, MA). These cells were then collected and placed in a 37°C 5% CO_2 humidified incubator for at least 1 h before use. Cells treated under the scrape loading conditions maintain functionality and sufficient quantities can be recovered for biochemical analysis (28).

C3 Purification. C3 purification has been described in detail elsewhere (29). In brief, JM109 transformed with C3 plasmid pGEX2T-C3 (provided by Dr. L. Feig, Tufts University, Boston, MA) were incubated with isopropyl-β-D-thiogalactopyranoside (100 μg/ml) during exponential growth phase for 4 h. Bacteria were lysed in cold PBS containing 1 mg/ml lysozyme, 1% Triton X-100, 25% sucrose, 1 mM EDTA, 5 mM 2-mercaptoethanol, and 1 mM PMSF. After sonication and DNase I (100 μg/ml; Boehringer Mannheim Corp., Indianapolis, IN) treatment, the lysate was centrifuged and supernatant was added to glutathione-agarose beads (Amersham Pharmacia Biotechnology Inc.), which

were rotated overnight at 4°C. C3 was cleaved from washed beads with 30 NIH units of bovine α-thrombin (Sigma Chemical Co.) and concentrated using a Centricon-3 (Amicon Corp., Easton, TX). The purity of C3 preparations was determined by SDS-PAGE. Control buffer for scrape loading of C3 consisted of the buffers used here, including the appropriate concentration of bovine α-thrombin used in the purification of C3.

C3 Ribosylation. C3 was scrape loaded into PB T lymphocytes at a concentration of 50 μg/ml. After scrape loading, cells were transferred into 1.5-ml eppendorf tubes and incubated for 1 h at 37°C to allow ribosylation. Cells were then washed extensively in 1% BSA/PBS to remove any C3 not incorporated into the cells. Next, the cells were resuspended at 5×10^6 cells/ml in ice-cold sonication buffer (250 mM sucrose, 10 mM Hepes, pH 7.4, 1 mM EDTA, 5 mM $MgCl_2$, 1 mM dithiothreitol [DTT], 0.1 mM GTP, 1 μg/ml leupeptin, 1 μg/ml pepstatin A, 1 μg/ml aprotinin, and 1 mM PMSF) and sonicated for 10 s. After sonication, 100 μl of the mixture was added to 50 μl of 3× reaction buffer containing 150 mM Tris-HCl, pH 8.0, 30 mM thymidine, 3 mM DTT, 5 mM $MgCl_2$, and 0.3 mM GTP. To this mixture, 1.0 μg purified C3 and 2 μCi ^{32}[P]-NAD (Dupont-NEN, Boston, MA) were added. After incubation for 1 h at 37°C, SDS was added to 2% final wt/vol and this mixture was immersed in a boiling water bath for 10 min. Eight volumes of ice-cold ethanol was then added and these samples were kept at −20°C for at least 1 h. Precipitated proteins were pelleted and dissolved in SDS-PAGE sample buffer by boiling for 10 min. Samples were then subjected to 12.5% SDS-PAGE and analyzed by autoradiography.

T Cell Costimulation of Proliferation. Immobilization of mAb to Easy Wash Elisa plates (Corning Glass Works) was performed by first incubating 50 μl (1 μg/ml in 0.1 M $NaHCO_3$, pH 8.0) of anti-CD3 mAb OKT3 for at least 30 min at room temperature before the addition of 50 μl of anti-β1 integrin mAb 33B6 or anti-α4β1 integrin mAb 19H8 (both at 8 μg/ml). After at least 2 h at 37°C, plates were blocked with BSA (1%, wt/vol). Plates were washed extensively before use with RPMI-1640. Purified human peripheral blood T cells that had been scrape loaded with BSA (50 μg/ml)/buffer control or with C3 exoenzyme (50 μg/ml) were then plated (5×10^4 cells/well) onto the immobilized costimulatory mAb in complete media. Approximately 2–3 d after initial plating, cells were pulsed with 0.5 μCi ^{3}[H]thymidine (Amersham Pharmacia Biotech Inc., Piscataway, NJ) in 50 μl complete media. After a 24-h incubation period, cells were harvested onto glass fiber filter mats (Whatman Ltd, Maidston, UK) using a PHD cell harvester (Cambridge Technology Inc., Cambridge, MA). ^{3}[H]Thymidine incorporation was measured via standard liquid scintillation counting (Beckman LS2800; Beckman Instruments Inc., Fullerton, CA).

Single Cell Analysis of Intracellular Cytokine Accumulation and αβ-TCR Downregulation. PB T cells were plated in complete media supplemented with 4 μM monensin (Sigma Chemical Co.) in 12-well tissue culture plates for activation by PMA (10 ng/ml) and ionomycin (1 μg/ml), or in bacteriological petri dishes that had been precoated with Fn, anti-α4β1 mAb 19H8, anti-β1 mAb 33B6, or anti-CD28 mAb Leu28 (10 μg/ml in 0.1 M $NaHCO_3$, pH 8.0), all in conjunction with the anti-CD3 mAb OKT3 (1 μg/ml in 0.1 M $NaHCO_3$). After 6 h, cells were harvested and intracellular cytokine production was measured. For the measurement of αβ-TCR downregulation, monensin was omitted from the culture medium. In brief, cells were washed once in stain/wash buffer (1% FBS and 0.1% NaN_3 in PBS). Directly conjugated antibodies to CD4 (see Figs. 6 and 7) or the αβ-TCR (see Fig. 8) were added, incubated for 30 min at 4°C, then washed in stain/wash buffer. Cells were fixed in 2% (wt/vol) paraformaldehyde overnight at 4°C, then permeabilized by washing once and resuspending with 0.1% (wt/vol) saponin (Sigma Chemical Co.), 1% FBS, and 0.1% NaN_3 in PBS (permeabilization buffer). Directly conjugated anti–IL-2 mAb was then added. After 30 min at 4°C, cells were again washed in permeabilization buffer two times, once in stain/wash buffer, and then read on an Epics Profile flow cytometer (Coulter Immunology). Control staining was performed with directly conjugated isotype and fluorochrome-matched immunoglobulin and then a minimum of 2×10^4 events were counted per test sample.

F-Actin Staining. PB T cells that had been scrape loaded with BSA (50 μg/ml) or C3 (50 μg/ml) were incubated in modified Tyrodes buffer on glass coverslips that had been precoated with Fn (10 μg/ml, in Tris-HCl, pH 9.5). Adherent PB T cells were then fixed overnight at 4°C in 2% paraformaldehyde. After fixation, cells were then treated with 0.1% Triton X-100 in PBS for 1 h at 4°C. Cells were then washed and incubated with 0.8 μM TRITC-phalloidin for 2 h at 4°C in PBS containing 1% FBS. After washing, coverslips were air dried and mounted in n-propyl gallate (2% wt/vol) in glycerol containing 10% PBS and then visualized on a Nikon Diaphot TMD inverted microscope.

Results and Discussion

C3 Induces ADP-Ribosylation of Rho in Human PB T Cells. Western blotting analysis confirmed the presence of RhoA (~25 kD) in the Jurkat variant J45.01 and PB T cells (Fig. 1 *A*). To study the role played by Rho in PB T cells we developed a technique allowing intracellular incorporation of macromolecules into freshly isolated T cells that maintains their functional cellular integrity and allows recovery of quantities of cells sufficient for biochemical analyses (28). This technique involves scrape loading T cells that are firmly adherent to the nonspecific cell attachment factor poly-L-lysine. After scrape loading BSA (50 μg/ml) as a control or C3 exoenzyme (50 μg/ml), cells were incu-

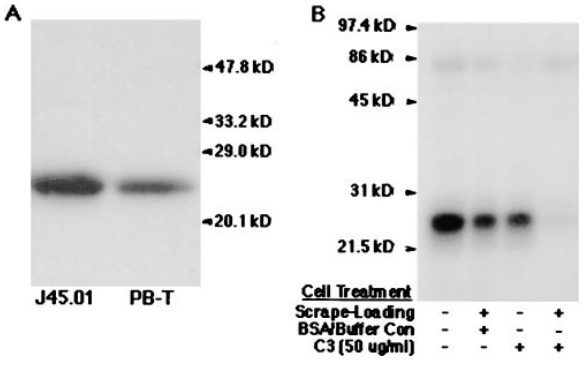

Figure 1. (*A*) Western blot of RhoA protein in whole cell lysates of the T cell line J45.01 and purified PB T lymphocytes. (*B*) Scrape loading efficiently incorporates enough C3 into freshly isolated, highly purified PB T lymphocytes for full ribosylation of Rho. Purified resting PB T cells were untreated (lane *1*), scrape loaded with 50 μg/ml BSA and control buffer (lane *2*), non-scrape loaded but incubated in the presence of C3 (50 μg/ml, lane *3*), or scrape loaded in the presence of C3 (50 μg/ml, lane *4*). See Materials and Methods for ribosylation reaction. Equal cell equivalents were loaded per lane. One of two representative experiments is shown.

bated for 1 h at 37°C to allow in vivo ribosylation. Cells were then washed thoroughly, sonicated, and lysates subjected to further C3 ribosylation by the addition of 2 μCi ^{32}[P]-NAD and 1 μg of C3 in ribosylation buffer. If full ribosylation of Rho proteins occurred before cell lysis due to effective C3 incorporation, then Rho would not be further ADP-ribosylated using ^{32}[P]-NAD as the ADP-donor (30). As Fig. 1 *B* demonstrates, scrape loading was a very effective procedure for incorporating C3 into PB T cells. Cells that were scrape loaded with BSA control (Fig. 1 *B*, lane *2*), or cells that were not plated on poly-l-lysine but incubated in the presence of C3 (Fig. 1 *B*, lane *3*), both could be further ribosylated by C3 in vitro after cell lysis. However, scrape loading of C3 (50 μg/ml) and thus causing in vivo ribosylation before cell lysis was very efficient as no further in vitro ribosylation of Rho occurred after cell disruption (Fig. 1 *B*, lane *4*).

Rho Differentially Regulates β1 and β2 Integrin-dependent Adhesive Interactions in PB T Lymphocytes. Freshly isolated resting PB T cells generally demonstrate low adhesion to β1 integrin substrates such as the extracellular matrix component Fn (31). However, adhesion can be augmented by various agents that seem to act by distinct methods. PMA can increase integrin-dependent cellular interactions not necessarily by increasing integrin affinity, but by events that strengthen intracellular integrin–cytoskeletal contacts and, thus, increase overall cellular avidity (26). Mn^{++}, on the other hand, binds to divalent cation binding sites in the extracellular regions of integrins and causes a conformational change into a high affinity form also resulting in increased cellular adhesion (32). As demonstrated in Fig. 2 *A*, basal adhesion of PB T cells to Fn was <10%, and this was dependent on α4β1 and α5β1 integrins (data not shown). Baseline adhesion was not inhibited by the ADP-ribosylation of Rho in C3 scrape-loaded cells (Fig. 2 *A*). Upregulation of PB T cell adhesion to Fn induced by PMA (10 ng/ml) or Mn^{++} (1 mM) was also unaffected by C3 treatment (Fig. 2 *A*). Like basal adhesion, PMA-induced adhesion was maximally inhibited with a combination of mAb specific for integrins α4β1 and α5β1, for both BSA scrape-loaded control cells and C3 scrape-loaded cells (Fig. 2 *B*). In summary, active Rho is not required for baseline or upregulated PB T cell adhesion to Fn mediated by phorbol ester or Mn^{++}.

Previous studies have shown that phorbol ester induction of B lymphoblastoid adhesion to vascular cell adhesion molecule 1 (mediated through α4 integrins; reference 33) can be inhibited in a dose-dependent manner by C3 exoenzyme (14), and NIH 3T3 cells microinjected with C3 detach from β1 integrin substrate (34). Conversely, inactivation of Rho in monocytes can promote integrin α5β1-dependent adhesion to Fn (35). In fact, elongation of the neuronal cell growth cone (38) and extension of dendritic like pseudopodial processes in T cell lines plated on β1 integrin substrates occurs upon inactivation of Rho (data not shown). According to models of cellular motility, pseudopod extension requires de novo formation of adhesive sites (36, 37), implying that in neuronal cells and PB T cells, inactivation of Rho does not prevent the formation of adhesive contacts. Thus it appears that Rho regulation of integrin adhesion is unique to the cellular background within which Rho is studied.

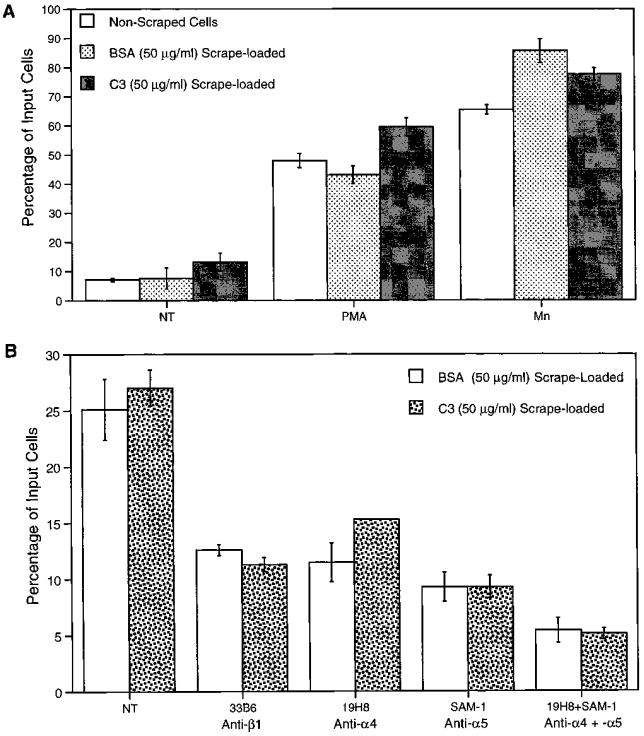

Figure 2. (*A*) ADP-ribosylation of Rho in PB T cells does not alter adhesion to Fn. An adhesion assay using untreated PB T cells, PB T cells scrape loaded with BSA (50 μg/ml) + control buffer, and C3 (50 μg/ml) scrape-loaded PB T cells, was performed. PMA (10 ng/ml) or Mn^{++} (1 mM) were added at the beginning of the assay to upregulate adhesion to Fn. One out of four representative experiments is shown. (*B*) Adhesion to Fn was tested in the presence of various mAb (10 μg/ml) to integrin subunits. Open bars represent BSA (50 μg/ml) scrape-loaded control cells. Stippled bars represent C3 exoenzyme (50 μg/ml) scrape-loaded test cells. Bars represent quadruplicate determinations and are expressed as the average ± SEM. One out of three representative experiments is shown.

Although inactivation of Rho in PB T cells does not affect adhesion to the β1 integrin substrate Fn as regulated by PMA or Mn^{++}, it does inhibit PMA-dependent homotypic aggregation (Fig. 3). Treatment of resting PB T cells with PMA induces the formation of cellular aggregates, as seen in the BSA scrape-loaded control cells (Fig. 3 *C*), whereas scrape loading C3 exoenzyme into PB T cells inhibits the formation of large aggregates (Fig. 3 *D*). This is similar to previous reports in B cell lines, where treatment with C3 inhibits PMA-induced αLβ2/intracellular adhesion molecule (ICAM)–dependent homotypic aggregation (13). C3-treated PB T cells still have the ability to aggregate, as an activating antibody specific for integrin αL, mAb 85G1, can overcome the inhibitory effects of C3 and induce aggregate formation (data not shown). Also, as aggregation progresses over 18–24 h, PMA-induced aggregation of the C3-treated cells approximates that of control BSA scrape-loaded cells (data not shown). This suggests

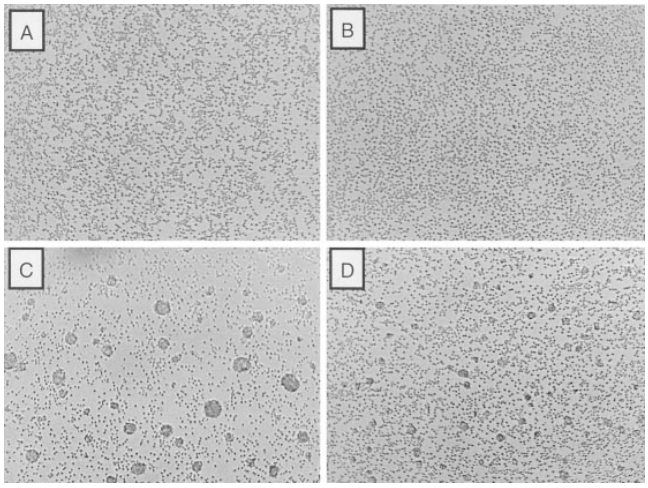

Figure 3. Inactivation of Rho inhibits PMA induced PB T cell homotypic aggregation. Cells were scrape loaded with BSA/buffer control (50 μg/ml, *A* and *C*), or C3 (50 μg/ml, *B* and *D*) as described in the Materials and Methods. Cells were not treated (*A* and *B*) or PMA treated (10 ng/ml, *C* and *D*) and then incubated for 4 h at 37°C. Initial magnification was 100×. One of three representative experiments is shown.

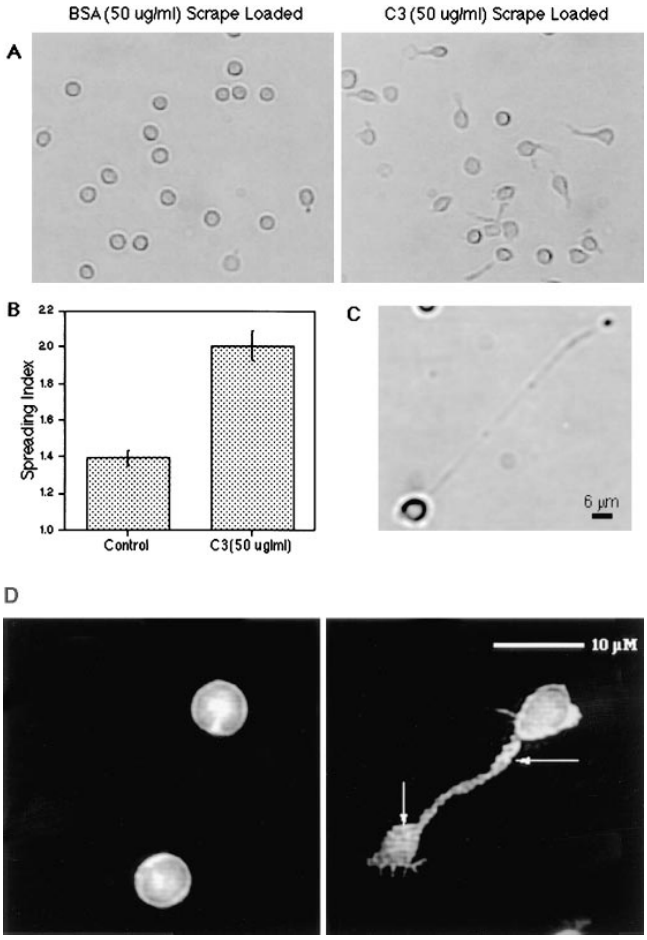

Figure 4. C3 ADP-ribosylated PB T cells extend pseudopodia when adherent to Fn. (*A*) Under similar conditions of the cell adhesion assays (see Materials and Methods), images of Fn adherent cells that had been scrape loaded with BSA (50 μg/ml) and buffer controls (scrape loading control) or cells that had been scrape loaded with C3 (50 μg/ml) were obtained. One of three representative experiments is shown. (*B*) Images were collected to quantitate (see Materials and Methods) the spreading index for control and C3-treated Fn adherent PB T lymphocytes. (*C*) An example of a cell that continued to elongate after a 4-h time period. Projections were up to nine times (in length) the width of a single cell. (*D*) Filamentous actin staining in C3-treated PB T cells adherent to Fn. Cells were either scrape loaded with BSA (50 μg/ml, *left*) or C3 (50 μg/ml, *right*) then plated in modified Tyrodes buffer on glass coverslips that had been coated with Fn (10 μg/ml). After 2 h, adherent cells were fixed in 2% paraformaldehyde and stained with TRITC-phalloidin. Arrows in the right panel represent clusters of filamentous actin in the extended pseudopods.

that the kinetics of PMA-induced aggregation are slower in the presence of C3. PMA-induced homotypic aggregation is a dynamic process, which in PB T cells predominantly involves integrin αLβ2/ICAM interactions (data not shown). In contrast, PB T cell adhesion to Fn can be mediated by α4β1 interaction with the alternatively spliced connecting segment-1 sequence EILDV (39) and/or via the canonical Fn receptor α5β1 interaction with RGD sequences (40). If β2 integrin–dependent homotypic aggregation can be equated with β1 integrin–dependent adhesion to Fn, then the above results suggest that Rho may differentially regulate β2 and β1 integrins within PB T cells. It will be interesting to determine if Rho plays a role in the complex pathways regulating a variety of recently described integrin related phenomena, such as transdominant regulation of integrin activity, whereby engagement of one integrin can regulate the function of other heterologous integrins (25, 41–45), or in the sequential solicitation of integrin α4β1 and α5β1 in monocyte adhesion to Fn induced by the CC chemokines MIP1-α or RANTES (46).

ADP-ribosylation of Rho in PB T Cells Causes F-Actin–rich Pseudopodial Extension on Fn Adherent Cells Without Any Prior Cellular Activation. Although the inhibition of Rho activity by C3 exoenzyme did not prevent constitutive or upregulated cell adhesion to the matrix component Fn, what was striking was the profound influence that scrape loading C3 exoenzyme had on the morphology of Fn adherent PB T cells. Adherent resting PB T cells generally remain round (Fig. 4 *A*, *left*). By scrape loading C3 alone, pseudopodial extension occurs without any prior T cell stimulation (Fig. 4 *A*, *right*). This morphological change occurred within 1 h of T cell plating and is quantitated in Fig. 4 *B*. Fn adherent C3-treated cells on average have a morphological index of 2.01 ± 0.08, whereas Fn adherent control PB T cells have a morphological index of 1.39 ± 0.04 (Fig. 4 *B*). This represents a 259.0% change from roundness (see Materials and Methods for formula) in the C3-treated cells. Aberrant pseudopodial extension continued well past the 1-h time point documented in Fig. 4, *A* and *B*, and extensions drastically elongated over time. In some instances, after 4 h these altered pseudopods were approximately nine times the width of a single cell (Fig. 4 *C*).

The extended pseudopods of the C3-treated PB T cells contained filamentous actin, some of which was in small punctate clusters (Fig. 4 *D*, *arrows*), which may represent coalescing actin cables such as those recently described in

monocyte cell lines (20). The GTPase Rho has been implicated in the regulation of actin filament assembly (10, 11). Rho has been shown to be required for phosphatidylinositol 4-phosphate 5-kinase (PIP 5-kinase) function in mouse fibroblasts (47), which is involved in the production of phosphatidylinositol 4,5-bisphosphate (4,5-PIP_2). It is interesting to speculate that dysregulated 4,5-PIP_2 levels could be responsible for pseudopodial extension in Fn adherent PB T cells that have been treated with C3. Actin filament nucleation and/or elongation may occur due to steady state levels of 4,5-PIP_2 being altered because a variety of cytoskeletal proteins involved in regulating cell morphology have been shown to interact with, or be regulated by, 4,5-PIP_2 (for review see reference 48). Also, pseudopodial extension in C3-treated PB T cells may be a manifestation of the apparent dichotomy in activity between Rho and other GTPases such as Cdc42, as demonstrated in neuronal cells (38).

ADP-Ribosylation of Rho Results in Inhibition of β1 Integrin-mediated Costimulation of Proliferation. PB T cells can be considered specialized sensory cells that seek out encounters with APC at nodal sites of antigen load, where productive engagement results in proper immune responses. Molecular mechanisms regulating locomotory machinery and maintaining T cell polarization in migrating cells inherently regulate T cell activation (8, 9, 49). Morphological changes may be linked to T cell activation as cytoskeletal regulatory proteins such as gelsolin can modulate phospholipase C (PLC) activity by competing for binding to PLCs preferred substrate, 4,5-PIP_2 (50). It is interesting then that besides the morphological changes regulated by GTPases of the Rho subfamily, a number of studies in other cell types have demonstrated that these GTPases are involved in the control of gene expression (51) and cell cycle progression (52). Since ADP-ribosylation of Rho by C3 exoenzyme results in such profound morphological changes in resting PB T cells, it was important to determine the effect C3 may have on their activation. Costimulation of proliferation can be accomplished in PB T cells by delivering signals through the TCR–CD3 complex in conjunction with signals generated through costimulatory molecules such as integrins (53–59). Costimulation assays were performed comparing cells that were scrape loaded with BSA (50 μg/ml, as a control) to those that were scrape loaded with C3 (50 μg/ml). To negate transitory effects that inhibition of Rho activity may have had on T cell adhesion to Fn not detected previously in the adhesion assays, mAb specific to integrin subunits were used as the costimulatory signal instead of Fn. In Fig. 5 it is clear that ADP-ribosylation of Rho has a dramatic effect on integrin-dependent T cell costimulation. β1 (mAb 33B6) and α4β1 (mAb 19H8) integrin induced costimulation of T cell proliferation was drastically inhibited, from 30,268 to 12,890 cpm and 20,185 to 9,336 cpm, respectively. Inhibition of integrin-mediated costimulation of proliferation as measured by DNA synthesis could occur by a number of mechanisms before entry into S phase of the cell cycle. In T lymphocytes, mitogenic signaling induced by the primary T cell growth factor IL-2 leads to inactivation of $p27^{kip}$ (60). Degradation of $p27^{kip}$ is required for G1 to S transition (61, 62). Inactivation of Rho proteins by C3 transferase in Rat FRTL-5 cells inhibits the degradation of $p27^{kip}$ (62). Also, inactivation of Rho proteins in a gastric derived tumor cell line results in decreased cyclin A expression (29), which is required for transition from the G1 to S phase of the cell cycle (63). Inhibiting DNA synthesis in PB T cells by inactivation of Rho could occur by either of these cell cycle–related processes. However, IL-2 is the main cytokine produced that induces T cells to cycle into S phase and synthesize DNA upon β1 integrin costimulation (57). So, inactivation of Rho could be preventing induction of IL-2 synthesis at very early stages in PB T cell activation.

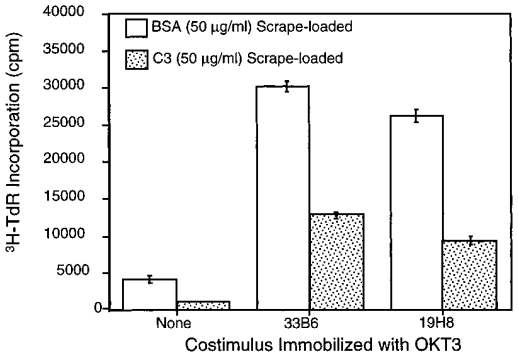

Figure 5. ADP-ribosylation of Rho inhibits β1 integrin-mediated costimulation of proliferation in PB T lymphocytes. Purified PB T lymphocytes that were either scrape loaded with control buffer + BSA (50 μg/ml), or with C3 transferase (50 μg/ml), were plated onto 96-well plates that had been precoated with OKT3 alone, or OKT3 coimmobilized with anti-β1 integrin mAb 33B6 or the anti-α4β1 integrin mAb 19H8. DNA synthesis was determined as described in the experimental procedures.

Inactivation of Rho Prevents Induction of IL-2 Production from β1 Integrin/CD3- or CD28/CD3-costimulated PB T Cells, but Not PMA- and Ionomycin-stimulated Cells. To test the hypothesis that inhibition of T cell activation by ADP-ribosylation of Rho was occurring at very early stages in T cell activation, an assay for the measurement of intracellular cytokine accumulation was used that can detect induction of cytokine synthesis at the single cell level using FACS® analysis (64) very early in T cell activation (28). The majority of cells producing IL-2 when costimulated by the coimmobilization of FN and anti-CD3 mAb are of the $CD4^+$ phenotype (Woodside, D.G, D.E Long, and B.W. McIntyre, manuscript submitted for publication). Hence, IL-2 measurements were obtained from $CD4^+$ cells that had been scrape loaded with BSA or C3 (50 μg/ml), then plated on bacteriological petri dishes that had been precoated with costimulatory substrate (Fn, 10 μg/ml) or mAbs (33B6 or 19H8, 10 μg/ml) in conjunction with anti-CD3 mAb OKT3. Cells were activated for 6 h in the presence of 4 μM monensin, as this has been predetermined to represent the time at which maximal intracellular IL-2 accumulation occurs (28). As Fig. 6 *A* demonstrates, ADP-ribosylation of Rho by scrape loading of C3 exoenzyme

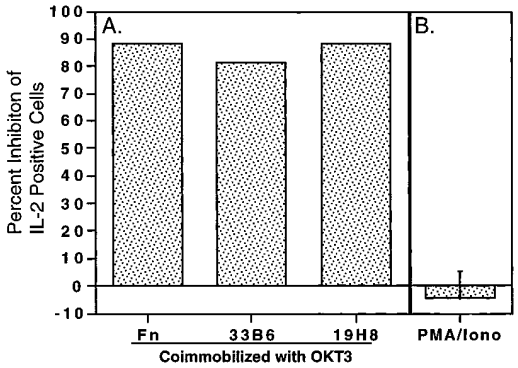

Figure 6. ADP-ribosylation of Rho protein inhibits early intracellular IL-2 accumulation in PB T cells as determined by FACS® analysis at the single cell level. (*A*) PB T cells were scrape loaded with control buffer + BSA (50 μg/ml) or with C3 transferase (50 μg/ml), and IL-2 was measured after 6 h of costimulation on plates coated with Fn, mAb 33B6 (anti-β1 integrin), or mAb 19H8 (anti-α4β1 integrin) coimmobilized with anti-CD3 mAb OKT3. Because the $CD4^+$ population preferentially coactivated due to integrin costimulation (data not shown), inhibition values were calculated from the $CD4^+$ population only. The percent inhibition in IL-2 positive cells was calculated from one of three representative experiments. (*B*) Costimulation of IL-2 production was measured by FACS® analysis for the entire population of PB T cells activated with PMA (10 ng/ml) and ionomycin (1 μM). Cells were scrape loaded with control buffer + BSA (50 μg/ml) or with C3 transferase (50 μg/ml) before activation and the IL-2 measured after 6 h of costimulation. Data represents the averages ± SEM from four separate donors. For parts *A* and *B*, the percent inhibition in IL-2 positive cells was calculated as $[1 - (\text{IL-2}^+_{\text{C3 SCRAPE}}/\text{IL-2}^+_{\text{BSA SCRAPE}})] \times 100$, where $\text{IL-2}^+_{\text{C3 SCRAPE}}$ = percentage of cells positive for intracellular IL-2 when scrape loaded with C3 and $\text{IL-2}^+_{\text{BSA SCRAPE}}$ = percentage of cells positive for intracellular IL-2 when scrape loaded with BSA + control buffer.

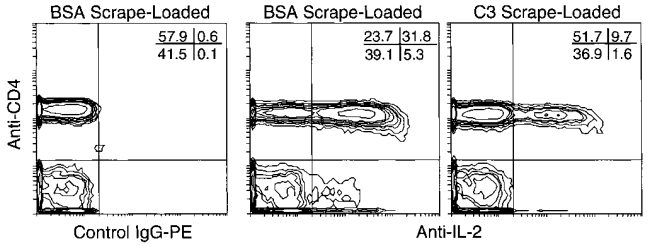

Cell Subtype	% IL-2 Positive		% Inhibition of IL-2 Production
	BSA Scraped	C3 Scraped	
$CD4^-$	11.9	4.2	65.1
$CD4^+$	57.3	15.9	72.2

Figure 7. Inactivation of Rho proteins inhibits CD28/CD3 induction of IL-2 production. PB T cells scrape loaded with BSA (50 μg/ml) in control buffer or C3 (50 μg/ml) were plated on bacteriological petri dishes for 6 h in the presence of 4 μM monensin. CD4 and intracellular IL-2 was stained as described in the experimental procedures and measured by FACS® analysis. At least 2×10^4 events were counted per test. One representative experiment of four is shown. Left panel represents IgG-PE control staining for intracellular IL-2. Middle and right panels represent IL-2 production in BSA (50 μg/ml) scrape-loaded control cells and C3 (50 μg/ml) scrape-loaded cells, respectively. Quadrate statistics are shown in the upper right corner of each panel. Percent inhibition as presented in the underlying chart was calculated as shown in Fig. 6 legend.

inhibited the intracellular production of IL-2 induced by costimulation through β1 integrins and CD3, by at least 81%. Unactivated cells, and cells that were plated on OKT3 alone did not demonstrate any significant production of IL-2 (data not shown). ADP-ribosylation of Rho had very little effect on intracellular IL-2 accumulation when PMA (10 μg/ml) and ionomycin (1 μM) were used to activate T cells, as there was an average 4.4% increase in IL-2 positive cells after C3 treatment (Fig. 6 *B*).

Since inactivation of Rho was specifically preventing integrin/CD3 costimulation of IL-2 production (but not PMA/ionomycin costimulation), we tested another costimulation scheme for the requirement of Rho activity. PB T cells were plated on anti-CD28 and -CD3 mAbs in complete media supplemented with 4 μM monensin. After 6 h activation, intracellular IL-2 was measured in the BSA (50 μg/ml) control scrape-loaded cells and the C3 (50 μg/ml) scrape-loaded cells. As demonstrated in Fig. 7, inactivation of Rho by scrape loading C3 inhibits CD28/CD3 costimulation of IL-2 production by at least 70% in $CD4^+$ T cells.

Downregulation of the αβ-TCR Is Unaffected by Inactivation of Rho in PB T Cells. Next we tested whether other receptor mediated events would be impaired upon the inactivation of Rho with C3 exoenzyme. Ligation of the TCR is associated with its internalization and thus downregulation from the cell surface (65, 66). To test if this was affected by C3 treatment, we took advantage of the ability to measure intracellular accumulation of IL-2 while simultaneously monitoring cell surface expression of the αβ-TCR at the single cell level. Control (BSA scrape loaded) and test cells (C3 scrape loaded) were treated under various activation conditions. Cells were then harvested and stained for the αβ-TCR, fixed in paraformaldehyde, solubilized with saponin, and stained for intracellular IL-2. The results are presented in Fig. 8. As expected, C3 treatment of peripheral blood lymphocytes inhibited CD28/CD3-dependent costimulation of IL-2 production, by 43% (Fig. 8 *A*). The percentage of cells positive for IL-2 in this experiment was relatively low as compared with that reported in Fig. 7. This is due to the absence of the Golgi disrupting agent monensin. It was unclear what affect monensin would have on normal intracellular trafficking and cell surface expression of the αβ-TCR–CD3 complex, so it was not included in these experiments. In part C of Fig. 8 the upper panels contain αβ-TCR expression histograms for BSA scrape-loaded PB T cells (controls). The lower panels contain αβ-TCR expression histograms for C3 scrape-loaded cells. As can be seen, even though there was >40% inhibition in the percentage of cells positive for IL-2 after C3 treatment (Fig. 8 *A*), there was no change in these cells due to treatment with C3 when cell surface expression of the αβ-TCR was examined. For example, when CD28 was cross-linked alone, the αβ-TCR mean fluorescence intensity was 11.3 and 11.6 for BSA and C3 scrape-loaded cells, respectively. When the CD3 complex was cross-linked with immobilized mAb OKT3, cell surface expression of the αβ-TCR decreased slightly, but again the mean fluorescence intensity for BSA- or C3-treated cells was almost identical (10.5 and 10.4, respectively). When both CD28 and CD3 were cross-linked at the same time with immobilized mAb, the

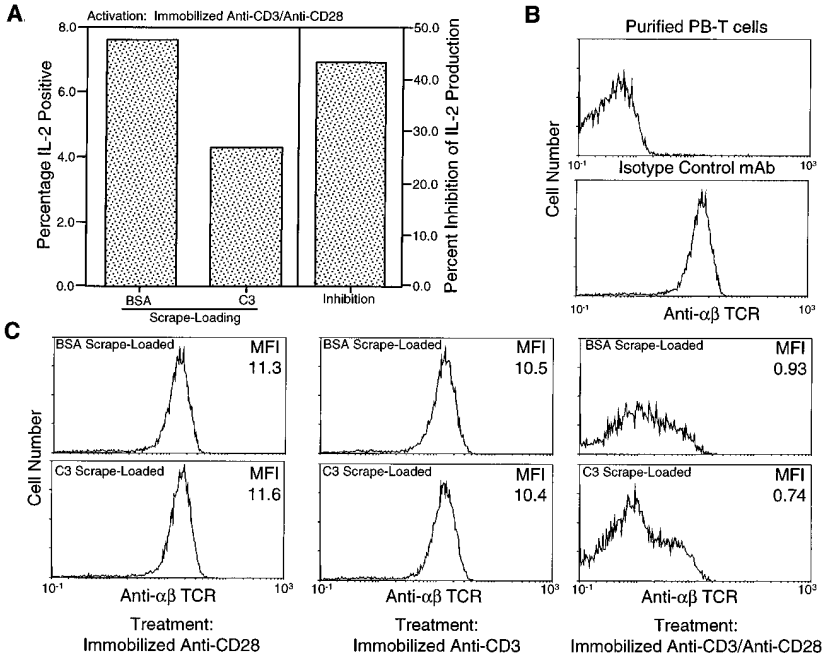

Figure 8. Cell surface expression of the αβ-TCR and intracellular staining of IL-2. (*A*) Control (BSA scrape loaded, 50 μg/ml) and test cells (C3 scrape loaded, 50 μg/ml) were activated with immobilized anti-CD28 and anti-CD3 in the absence of monensin, harvested, and intracellular staining for IL-2 was performed after staining for the αβ-TCR as described in the Materials and Methods. (*B*) Control staining for αβ-TCR expression on BSA scrape-loaded PB T cells. (*C*) Cells were treated under the various conditions indicated then stained for the αβ-TCR. The upper panels of histograms represent cells scrape loaded with BSA (50 μg/ml), and the lower panels of histograms represent C3 exoenzyme (50 μg/ml) scrape-loaded PB T cells. The last column of histograms (treated with anti-CD28 and anti-CD3 mAbs) were the same population of cells that were stained for intracellular IL-2 accumulation in *A*. This is representative of two experiments performed with similar results.

mean fluorescence intensity of the αβ-TCR decreased logarithmically. The αβ-TCR mean fluorescence intensity of BSA scrape-loaded cells was 0.93, and the mean fluorescence intensity of C3 scrape-loaded cells was 0.74. Again, there was little difference between the downregulation of TCR expression on C3 treated or control cells due to costimulatory signals. To summarize, receptor-mediated TCR downregulation was unaffected by C3 treatment of PB T cells even though C3 treatment did inhibit IL-2 production by >40% in the same cell population.

Both β1 integrin and CD28 costimulation of PB T cell IL-2 production require functional Rho. One possible explanation of this is that Rho is regulating a common signaling pathway used by both these costimulatory molecules. Costimulatory signals such as those delivered by integrins in PB T cells have been compared with adhesion dependent signals required for anchorage dependent growth in fibroblast models, which are thought to provide substrate for enzymes activated by growth factors (67). As previously mentioned, Rho activity is required for PIP5-K–dependent production of 4,5-PIP_2 (47), which is the preferred substrate for PLC. Cleavage of 4,5-PIP_2 by PLC results in the production of diacylglycerol (DAG), and inositol triphosphate (IP_3; for review see reference 68), both of which have been implicated in PB T cell activation (for review see reference 69). Expanding upon the anchorage-dependent growth analogy in PB T cells treated with C3 exoenzyme, TCR signals activating PLC would be unproductive with regard to cellular activation as inactive Rho may not be sufficiently regulating levels of the PLC substrate 4,5-PIP_2. Since PMA activation of PKC (70) and ionomycin-mediated Ca^{++} release are thought to mimic the effects of the products of the lipase activity of PLC on 4,5-PIP_2, namely DAG and IP_3, our finding that PMA and ionomycin costimulation overcomes the C3 inhibitory effects support a role for Rho in the regulation of 4,5-PIP_2 in PB T cells. Consistent with this is the recent finding that transient cytosolic Ca^{++} increases induced by Fc receptor cross-linking in monocytes diminished after C3 microinjection (71).

Alternatively, as the common denominator between costimulatory pathways involving CD28/CD3 and β1 integrin/CD3 is cross-linking the CD3 complex, it is also possible that Rho activity is required for initiation or propagation of TCR/CD3-specific signals. In this regard, it has recently been demonstrated by Han et al. (72) that the src tyrosine kinase lck regulates vav activity. Phosphorylated vav, which has a Dbl homology domain thought to be responsible for guanine nucleotide exchange activity (73, 74), has been implicated as a guanine nucleotide exchange factor for Rho family GTPases (72). If this is the case in PB T cells, where the importance of lck activity is well documented (for review see reference 75), activation of Rho may be a key component of the TCR signal transduction process.

That Rho may be a participant in costimulatory signals or in TCR signals alludes to a third possibility. Rho could be at a point of convergence or at the crossroads of TCR and costimulatory molecule signaling mechanisms as Rho activity could influence other GTPases important in PB T cell activation. For example, phosphorylated p120 Ras GTPase-activating protein (Ras-GAP) complexes with phosphorylated p190 Rho-GAP (76–78). Dysregulation of Rho activity could interfere with Ras-GAP/Rho-GAP interactions, causing increased or accelerated Ras-GTPase activity effectively blocking Ras-dependent signaling pathways.

This is the first demonstration that Rho activity is required in T lymphocyte activation and the maintenance of normal T lymphocyte cytoarchitecture as inactivation of Rho results in inhibition of IL-2 production and causes pseudopodial extension in quiescent primary T lymphocytes. Determination of cytoskeletal regulatory elements, signaling modules, and transcriptional factors affected when Rho-inactivated T cells are costimulated will be an important area of future study, as it may lead to novel strategies to therapeutically regulate immune function by influencing T lymphocyte activity on at least two different levels, migration and/or activation.

We would like to thank J.N. Wygant for technical assistance.

This work was supported by grant CA62596 from the National Institutes of Health.

Address correspondence to Brad McIntyre, Department of Immunology, University of Texas M.D. Anderson Cancer Center, 1515 Holcombe Blvd., Box 180, Houston, TX 77030. Phone: 713-792-8739; Fax: 713-745-0846; E-mail: bmcintyr@notes.utmdacc.tmc.edu

Dr. Woodside's present address is Department of Vascular Biology, The Scripps Research Institute, La Jolla, CA 92037.

Received for publication 11 November 1997 and in revised form 9 June 1998.

References

1. Pardi, R., L. Inverardi, C. Rugarli, and J.R. Bender. 1992. Antigen-receptor complex stimulation triggers protein kinase C-dependent CD11a/CD18-cytoskeleton association in T lymphocytes. *J. Cell Biol.* 116:1211–1220.
2. Bourguignon, L.Y., S.J. Suchard, M.L. Nagpal, and J.R. Glenney. 1985. A T-lymphoma transmembrane glycoprotein (gp180) is linked to the cytoskeletal protein, fodrin. *J. Cell Biol.* 101:477–487.
3. Taffs, R.E., and S.J. Ewald. 1989. Concanavalin A induces a cytoskeletal association of T200 molecules in T lymphocytes. *Mol. Immunol.* 26:925–937.
4. Geppert, T.D., and P.E. Lipsky. 1991. Association of various T cell-surface molecules with the cytoskeleton. Effect of cross-linking and activation. *J. Immunol.* 146:3298–3305.
5. Caplan, S., S. Zeliger, L. Wang, and M. Baniyash. 1995. Cell surface-expressed T-cell antigen-receptor ζ chain is associated with the cytoskeleton. *Proc. Natl. Acad. Sci. USA.* 92:4768–4772.
6. Rozdzial, M.M., B. Malissen, and T.H. Finkel. 1995. Tyrosine-phosphorylated T cell receptor ζ chain associates with the actin cytoskeleton upon activation of mature T lymphocytes. *Immunity.* 3:623–633.
7. Caplan, S., and M. Baniyash. 1996. Normal T cells express two T cell antigen receptor populations, one of which is linked to the cytoskeleton via ζ chain and displays a unique activation-dependent phosphorylation pattern. *J. Biol. Chem.* 271:20705–20712.
8. Valitutti, S., M. Dessing, K. Aktories, H. Gallati, and A. Lanzavecchia. 1995. Sustained signaling leading to T cell activation results from prolonged T cell receptor occupancy. Role of T cell actin cytoskeleton. *J. Exp. Med.* 181:577–584.
9. Shaw, A.S., and M.L. Dustin. 1997. Making the T cell receptor go the distance: a topological view of T cell activation. *Immunity.* 6:361–369.
10. Ridley, A.J. 1995. Rho-related proteins: actin cytoskeleton and cell cycle. *Curr. Opin. Gen. Dev.* 5:24–30.
11. van Aelst, L., and C. D'Souza-Schorey. 1997. Rho GTPases and signaling networks. *Genes Dev.* 11:2295–2322.
12. Ridley, A.J., and A. Hall. 1992. The small GTP-binding protein rho regulates the assembly of focal adhesions and actin stress fibers in response to growth factors. *Cell.* 70:389–399.
13. Tominaga, T., K. Sugie, M. Hirata, N. Morii, J. Fukata, A. Uchida, H. Imura, and S. Narumiya. 1993. Inhibition of PMA-induced, LFA-1–dependent lymphocyte aggregation by ADP ribosylation of the small molecular weight GTP binding protein, rho. *J. Cell Biol.* 120:1529–1537.
14. Laudanna, C., J.J. Campbell, and E.C. Butcher. 1996. Role of rho in chemoattractant-activated leukocyte adhesion through integrins. *Science.* 271:981–983.
15. Koch, G., J. Norgauer, and K. Aktories. 1994. ADP-ribosylation of the GTP-binding protein rho by clostridium limosum exoenzyme affects basal, but not *N*-formyl-peptide-stimulated, actin polymerization in human myeloid leukaemic (HL-60) cells. *Biochem. J.* 299:775–779.
16. Ehrengruber, M.U., P. Boquet, T.D. Coates, and D.A. Deranleau. 1995. ADP-ribosylation of rho enhances actin polymerization-coupled shape oscillations in human neutrophils. *FEBS Lett.* 373:161–164.
17. Lang, P., L. Guizani, I. Vitte-Mony, R. Stancou, O. Dorseuil, G. Gacon, and J. Bertoglio. 1992. ADP-ribosylation of the ras-related, GTP-binding protein RhoA inhibits lymphocyte-mediated cytotoxicity. *J. Biol. Chem.* 267: 11677–11680.
18. Lang, P., F. Gesbert, M. Delespine-Carmagnat, R. Stancou, M. Pouchelet, and J. Bertoglio. 1996. Protein kinase A phosphorylation of RhoA mediates the morphological and functional effects of cyclic AMP in cytotoxic lymphocytes. *EMBO (Eur. Mol. Biol. Organ.) J.*15:510–519.
19. Aepfelbacher, M., M. Essler, E. Huber, A. Czech, and P.C. Weber. 1996. Rho is a negative regulator of human monocyte spreading. *J. Immunol.* 157:5070–5075.
20. Allen, W.E., G.E. Jones, J.W. Pollard, and A.J. Ridley. 1997. Rho, rac and cdc42 regulate actin organization and cell adhesion in macrophages. *J. Cell Sci.* 110:707–720.

21. Henning, S.W., R. Galandrini, A. Hall, and D.A. Cantrell. 1997. The GTPase Rho has a critical regulatory role in thymus development. *EMBO (Eur. Mol. Biol. Organ.) J.* 18: 2397–2407.
22. Hynes, R.O. 1993. Fibronectins. A. Rich, editor. Springer-Verlag, NY. p. 12.
23. Bednarczyk, J.L., M.C. Szabo, J.N. Wygant, A.I. Lazarovits, and B.W. McIntyre. 1994. Identification of a combinatorial epitope expressed by the integrin α4β1 heterodimer involved in the regulation of cell adhesion. *J. Biol. Chem.* 269:8348–8354.
24. Bednarczyk, J.L., J.N. Wygant, M.C. Szabo, L. Molinari-Storey, M. Renz, S. Fong, and B.W. McIntyre. 1993. Homotypic leukocyte aggregation triggered by a monoclonal antibody specific for a novel epitope expressed by the integrin β1 subunit: conversion of nonresponsive cells by transfecting human integrin α4 subunit cDNA. *J. Cell. Biochem.* 51:465–478.
25. Woodside, D.G., T.K. Teague, and B.W. McIntyre. 1996. Specific inhibition of T lymphocyte coactivation by triggering integrin β1 reveals convergence of β1, β2, and β7 integrin signaling pathways. *J. Immunol.* 157:700–706.
26. Faull, R.J., N.L. Kovach, J.M. Harlan, and M.H. Ginsberg. 1994. Stimulation of integrin-mediated adhesion of T lymphocytes and monocytes: two mechanisms with divergent biological consequences. *J. Exp. Med.* 179:1307–1316.
27. Szabo, M.C., T.K. Teague, and B.W. McIntyre. 1995. Regulation of lymphocyte pseudopodia formation by triggering the integrin α4β1. *J. Immunol.* 154:2112–2124.
28. Woodside, D.G., and B.W. McIntyre. 1998. Inhibition of CD28/CD3 mediated costimulation of naive and memory human T lymphocytes by intracellular incorporation of polyclonal antibodies specific for the AP-1 transcriptional complex. *J. Immunol.* 161:649–658.
29. Udagawa, T., and B.W. McIntyre. 1996. ADP-ribosylation of the G protein rho inhibits integrin regulation of tumor cell growth. *J. Biol. Chem.* 271:12542–12548.
30. Rubin, E.J., D.M. Gill, P. Boquet, and M.R. Popoff. 1988. Functional modification of a 21-kilodalton G protein when ADP-ribosylated by exoenzyme C3 of clostridium botulinum. *Mol. Cell. Biol.* 8:418–416.
31. Shimizu, Y., G.A. Van Seventer, K.J. Horgan, and S. Shaw. 1990. Regulated expression and binding of three VLA (β1) integrin receptors on T cells. *Nature.* 345:250–253.
32. Gailit, J., and E. Ruoslahti. 1988. Regulation of the fibronectin receptor affinity by divalent cations. *J. Biol. Chem.* 263: 12927–12932.
33. Chan, B.M., M.J. Elices, E. Murphy, and M.E. Hemler. 1992. Adhesion to vascular cell adhesion molecule 1 and fibronectin. Comparison of α4β1 (VLA-4) and α4β7 on the human B cell line JY. *J. Biol. Chem.* 267:8366–8370.
34. Paterson, H.F., A.J. Self, M.D. Garrett, I. Just, K. Aktories, and A. Hall. 1990. Microinjection of recombinant p21rho induces rapid changes in cell morphology. *J. Cell Biol.* 111: 1001–1007.
35. Aepfelbacher, M. 1995. ADP-ribosylation of Rho enhances adhesion of U937 cell to fibronectin via the α5β1 integrin receptor. *FEBS Lett.* 363:78–80.
36. Lauffenburger, D.A., and A.F. Horwitz. 1996. Cell migration: a physically integrated molecular process. *Cell.* 84:359–369.
37. Mitchison, T.J., and L.P. Cramer. 1996. Actin-based cell motility and cell locomotion. *Cell.* 84:371–379.
38. Kozma, R., S. Sarner, S. Ahmed, and L. Lim. 1997. Rho family GTPases and neuronal growth cone remodelling: relationship between increased complexity induced by Cdc42Hs, Rac1, and acetylcholine and collapse induced by RhoA and lysophosphatidic acid. *Mol. Cell. Biol.* 17:1201–1211.
39. Wayner, E.A., A. Garcia-Pardo, M.J. Humphries, J.A. McDonald, and W.G. Carter. 1989. Identification and characterization of the lymphocyte adhesion receptor for an alternative cell attachment domain in plasma fibronectin. *J. Cell Biol.* 109:1321–1330.
40. Pytela, R., M.D. Pierschbacher, and E. Ruoslahti. 1985. Identification and isolation of a 140 kd cell surface glycoprotein with properties expected of a fibronectin receptor. *Cell.* 40:191–198.
41. van Kooyk, Y., E. van de Wiel-van Kemenade, P. Weder, R.J.F. Huijbens, and C.G. Figdor. 1993. Lymphocyte function-associated antigen 1 dominates very late antigen 4 in binding of activated T cells to endothelium. *J. Exp. Med.* 177:185–190.
42. Blystone, S.D., I.L. Graham, F.P. Lindberg, and E.J. Brown. 1994. Integrin αvβ3 differentially regulated adhesive and phagocytic functions of the fibronectin receptor α5β1. *J. Cell Biol.* 127:1129–1137.
43. Blystone, S.D., F.P. Lindberg, S.E. LaFlamme, and E.J. Brown. 1995. Integrin β3 cytoplasmic tail is necessary and sufficient for regulation of α5β1 phagocytosis by αvβ3 and integrin-associated protein. *J. Cell Biol.* 130:745–754.
44. Huhtala, P., M.J. Humphries, J.B. McCarthy, P.M. Tremble, Z. Werb, and C.H. Damsky. 1995. Cooperative signaling by α5β1 and α4β1 integrins regulates metalloproteinase gene expression in fibroblasts adhering to fibronectin. *J. Cell Biol.* 129:867–879.
45. Diaz-Gonzalez, F., J. Forsyth, B. Steiner, and M.H. Ginsberg. 1996. Trans-dominant inhibition of integrin function. *Mol. Biol. Cell.* 7:1939–1951.
46. Weber, C., R. Alon, B. Moser, and T.A. Springer. 1996. Sequential regulation of α4β1 and α5β1integrin avidity by CC chemokines in monocytes: implications for transendothelial chemotaxis. *J. Cell Biol.* 134:1063–1073.
47. Chong, L.D., A. Traynor-Kaplan, G.M. Bokoch, and M.A. Schwartz. 1994. The small GTP-binding protein rho regulates a phosphatidylinositol 4-phosphate 5-kinase in mammalian cells. *Cell.* 79:507–513.
48. Jockusch, B.M., P. Bubeck, K. Giehl, M. Kroemker, J. Moschner, M. Rothkegel, M. Rudiger, K. Schluter, G. Stanke, and J. Winkler. 1995. The molecular architecture of focal adhesions. *Annu. Rev. Cell Dev. Biol.* 11:379–416.
49. Negulescu, P.A., T.B. Krasieva, A. Khan, H.H. Kerschbaum, and M.D. Cahalan. 1996. Polarity of T cell shape, motility, and sensitivity to antigen. *Immunity.* 4:421–430.
50. Sun, H.Q., K. Lin, and H.L. Yin. 1997. Gelsolin modulates phospholipase C activity in vivo through phospholipid binding. *J. Cell Biol.* 138:811–820.
51. Hill, C.S., J. Wynne, and R. Treisman. 1995. The Rho Family of GTPases RhoA, Rac1, and CDC42Hs regulate transcriptional activation by SRF. *Cell.* 81:1159–1170.
52. Olson, M.F., A. Ashworth, and A. Hall. 1995. An essential role for rho, rac, and cdc42 GTPases in cell cycle progression through G1. *Science.* 269:1270–1272.
53. Damle, N.K., and A. Aruffo. 1991. Vascular cell adhesion molecule-1 induces T-cell antigen receptor-dependent activation of CD4+ T lymphocytes. *Proc. Natl. Acad. Sci. USA.* 88:6403–6407.
54. Davis, L.S., N. Oppenheimer-Marks, J.L. Bednarczyk, B.W.

McIntyre, and P.E. Lipsky. 1990. Fibronectin promotes proliferation of naive and memory T cells by signaling through both the VLA-4 and VLA-5 integrin molecules. *J. Immunol.* 145:785–793.

55. Matsuyama, T., A. Yamada, J. Kay, K.M. Yamada, S.K. Akiyama, S.F. Schlossman, and C. Morimoto. 1989. Activation of CD4 cells by fibronectin and anti-CD3 antibody: a synergistic effect mediated by the VLA-5 fibronectin receptor complex. *J. Exp. Med.* 170:1133–1148.
56. Shimizu, Y., G.A. van Seventer, K.J. Horgan, and S. Shaw. 1990. Costimulation of proliferative responses of resting CD4+ T cells by the interaction of VLA-4 and VLA-5 with fibronectin or VLA-6 with laminin. *J. Immunol.* 145:59–67.
57. Udagawa, T., and B.W. McIntyre. 1992. A VLA-4 α-chain specific monoclonal antibody enhances CD3-induced IL-2/IL-2 receptor-dependent T-cell proliferation. *Lymphokine Cytokine Res.* 11:193–199.
58. van Seventer, G.A., Y. Shimizu, K.J. Horgan, and S. Shaw. 1990. The LFA-1 ligand ICAM-1 provides an important costimulatory signal for T cell receptor-mediated activation of resting T cells. *J. Immunol.* 144:4579-4586.
59. Bednarczyk, J.L., T.K. Teague, J.N. Wygant, L.S. Davis, P.E. Lipsky, and B.W. McIntyre. 1992. Regulation of T cell proliferation by anti-CD49d and anti-CD29 monoclonal antibodies. *J. Leuk. Biol.* 52:456–462.
60. Firpo, E.J., A. Koff, M.J. Solomon, and J.M. Roberts. 1994. Inactivation of a Cdk-2 inhibitor during interleukin-2 induced proliferation of human T lymphocytes. *Mol. Cell. Biol.* 14:4889–4901.
61. Polyak, K., M.H. Lee, H. Erdjument-Bromage, A. Koff, J.M. Roberts, P. Tempst, and J. Massague. 1994. Cloning of p27kip1, a cyclin-dependent kinase inhibitor and a potential mediator of extracellular mitogenic signals. *Cell.* 78:59–66.
62. Hirai, A., S. Nakamura, Y. Noguchi, T. Yasuda, M. Kitagawa, I. Tatsuno, T. Oeda, K. Tahara, T. Terano, S. Narumiya, et al. 1997. Geranylgeranylated rho small GTPase(s) are essential for the degradation of p27kip1 and facilitate the progression from G1 to S phase in growth-stimulated Rat FRTL-5 cells. *J. Biol. Chem.* 272:13–16.
63. Wang, J., X. Chenivesse, B. Henglein, and C. Brechot. 1990. Hepatitis B virus integration in a cyclin A gene in a hepatocellular carcinoma. *Nature.* 343:555–557.
64. Sander, B., J. Andersson, and U. Andersson. 1991. Assessment of cytokines by immunofluorescence and the paraformaldehyde-saponin procedure. *Immunol. Rev.* 119:65–93.
65. Zanders E.D., J.R. Lamb, M. Feldmann, N. Green, and P.C. Beverley. 1983. Tolerance of T-cell clones is associated with membrane antigen changes. *Nature.* 303:625–627.
66. Krangel, M.S. 1987. Endocytosis and recycling of the T3-T cell receptor complex. The role of T3 phosphorylation. *J. Exp. Med.* 165:1141–1159.
67. Schwartz, M.A., M.D. Schaller, and M.H. Ginsberg. 1995. Integrins: emerging paradigms of signal transduction. *Annu. Rev. Cell Dev. Biol.* 11:549–599.
68. Divecha, N., and R.F. Irvine. 1995. Phospholipid Signaling. *Cell.* 80:269–278.
69. Weiss, A., and D.R. Littman. 1994. Signal transduction by lymphocyte antigen receptors. *Cell.* 76:263–274.
70. Castagna, M., Y. Takai, K. Kaibuchi, K. Sano, U. Kikkawa, and Y. Nishizuka. 1982. Direct activation of calcium-activated phospholipid-dependent protein kinase by tumor-promoting phorbol esters. *J. Biol. Chem.* 247:7847–7851.
71. Hackam, D.J., O.D. Rotstein, A. Schreiber, W. Zhang, and S. Grinstein. 1997. Rho is required for the initiation of calcium signaling and phagocytosis by Fcγ receptors in macrophages. *J. Exp. Med.* 186:955–966.
72. Han, J., B. Das, W. Wei, L. Van Aelst, R.D. Mosteller, R. Khosravi-Far, J.K. Westwick, C.J. Der, and D. Broek. 1997. Lck regulates vav activation of members of the rho family of GTPases. *Mol. Cell. Biol.* 17:1346–1353.
73. Hart, M.J., A. Eva, T. Evans, S.A. Aaronson, and R.A. Cerione. 1991. Catalysis of guanine nucleotide exchange on the cdc42Hs protein by the dbl oncogene product. *Nature.* 354: 311–314.
74. Hart, M.J., A. Eva, D. Zangrilli, S.A. Aaronson, T. Evans, R.A. Cerione, and Y. Zheng. 1994. Cellular transformation and guanine nucleotide exchange activity are catalyzed by a common domain on the dbl oncogene. *J. Biol. Chem.* 269: 62–65.
75. Chan, A.C., D.M. Desai, and A. Weiss. 1994. The role of protein tyrosine kinases and protein tyrosine phosphatases in T cell antigen receptor signal transduction. *Annu. Rev. Immunol.* 12:555–592.
76. Ellis, C., M. Moran, F. McCormick, and T. Pawson. 1990. Phosphorylation of GAP and GAP-associated proteins by transforming and mitogenic tyrosine kinases. *Nature.* 343: 377–381.
77. Moran, M.F., P. Polakis, F. McCormick, T. Pawson, and C. Ellis. 1991. Protein-tyrosine kinases regulate the phosphorylation, protein interactions, subcellular distribution, and activity of p21ras GTPase-activating protein. *Mol. Cell. Biol.* 11:1804–1812.
78. Bryant, S.S., S. Briggs, T.E. Smithgall, G.A. Martin, F. McCormick, J.H. Chang, S.J. Parsons, and R. Jove. 1995. Two SH2 domains of p120 Ras GTPase-activating protein bind synergistically to tyrosine phosphorylated p190 Rho GTPase-activating protein. *J. Biol. Chem.* 270:17947–17952.